HHS Public Access

Author manuscript

Science. Author manuscript; available in PMC 2019 October 04.

Published in final edited form as:

Science. 2019 February 01; 363(6426): 538–542. doi:10.1126/science.aau8722.

Intense Threat Switches Dorsal Raphe Serotonin Neurons to a Paradoxical Operational Mode

Changwoo Seo[†,1,2], **Akash Guru**[†,1,2], **Michelle Jin**[‡,1], **Brendan Ito**[1], **Brianna J. Sleezer**[1], **Yi-Yun Ho**[1,2], **Elias Wang**[§,1], **Christina Boada**[¶,1], **Nicholas A. Krupa**[1], **Durgaprasad S. Kullakanda**[1], **Cynthia X. Shen**[1], **Melissa R. Warden**[1,2,*]

[1]Department of Neurobiology and Behavior, Cornell University, Ithaca, NY 14853, USA.

[2]Cornell Neurotech, Cornell University, Ithaca, NY 14853, USA.

Abstract

Survival depends on the selection of behaviors adaptive for the current environment. For example, a mouse should run from a rapidly looming hawk but should freeze if the hawk is coasting across the sky. Although serotonin has been implicated in adaptive behavior, environmental regulation of its functional role remains poorly understood. We found that stimulation of dorsal raphe serotonin neurons suppressed movement in low- and moderate-threat environments but induced escape behavior in high-threat environments, and that movement-related dorsal raphe serotonin neural dynamics inverted in high-threat environments. Stimulation of dorsal raphe GABA neurons promoted movement in negative but not positive environments, and movement-related GABA neural dynamics inverted between positive and negative environments. Thus, dorsal raphe circuits switch between distinct operational modes to promote environment-specific adaptive behaviors.

One Sentence Summary

Dorsal raphe serotonin neuron activity promotes opposite behaviors in high-threat and low-threat environments.

The decision to move or to refrain from movement depends on the structure of the environment and the internal state of the animal. Imminent threats may provoke a ‘fight-or-flight’ response, while distant or uncertain threats may induce either vigilant freezing or a

[*]Corresponding author. mrwarden@cornell.edu.
[‡]Current address: Neurobiology of Relapse Section, National Institute on Drug Abuse (NIDA) Intramural Research Program, Baltimore, MD 21224, USA.
[§]Current address: Department of Electrical Engineering, Stanford University, Stanford, CA 94305, USA.
[¶]Current address: School of Medicine, New York University, New York, NY 10016, USA.
[†]Equal contributors.

Author contributions: C.S. and M.R.W. conceived the project and designed the experiments; C.S., M.J., B.I., B.J.S., C.B., and N.A.K. performed stereotaxic surgery and histology; C.S., M.J., C.B., N.A.K., and D.K. conducted photometry and optogenetic experiments; A.G., B.I., B.J.S., and C.S. conducted single cell physiology experiments; C.S. and Y.Y.H. developed the behavioral data acquisition methods; C.S., A.G., B.J.S., M.J., E.W., C.X.S., and M.R.W. analyzed the data; C.S. and M.R.W. prepared the manuscript; M.R.W. supervised all aspects of the work.

Competing interests: The authors declare no competing financial interests.

Data and materials availability: All data are available in the manuscript or the supplementary materials.

delayed, strategic avoidance response (1, 2). Hunger may encourage travel to a distant food source, while a sated animal may not find this goal worth the energy expenditure or risk (3).

Neuromodulatory systems receive input from brain regions that represent environmental structure and internal state (4), and are essential for the coordinated regulation of the neural circuits that control movement. While dopamine (DA) promotes behavioral activation in vertebrates (5, 6), forebrain serotonin (5-hydroxytryptamine; 5-HT) is more strongly associated with behavioral inhibition (7, 8); elevated 5-HT promotes pausing and waiting (9–11), while reduced 5-HT promotes impulsivity and perseverative responding (12, 13). Paradoxically, selective serotonin reuptake inhibitors (SSRIs) reduce immobility in the forced swim test (FST) and tail suspension test (TST) (14), as does stimulation of the prefrontal-dorsal raphe nucleus (DRN) projection (15). We sought to investigate whether differences in environmental threat level underlie this discrepancy.

We used fiber photometry (16) to monitor the population dynamics of DRN 5-HT neurons in freely behaving mice (fig. S1A). We injected AAV5-CAG-FLEX-GCaMP6s (17) into the DRN of SERT-Cre mice (18), and implanted an optical fiber over the DRN (Fig. 1A and fig. S1B). Movement onset in the open field test (OFT, Fig. 1B) was associated with a robust reduction in DRN 5-HT fluorescence (Fig. 1, C to E; GFP control data, Fig. 1E and fig. S1, C to E). We then recorded DRN 5-HT activity during performance of a cued reward approach task (Fig. 1F and fig. S2, A and B), in which mice crossed an operant chamber to receive a reward, and found that activity decreased on movement in this environment (Fig. 1, G to I; movement offset, fig. S3, A and B). We also found that DRN 5-HT activity decreased on movement to avoid a shock in a cued avoidance task (Fig. 1, J to M, and fig. S2, C and D; movement offset, fig. S3, C and D).

Next, we examined DRN 5-HT neural activity during the TST (Fig. 2A), a high-threat environment (19), and observed an increase in DRN 5-HT fluorescence on movement onset (Fig. 2, B to D; GFP data, Fig. 2D and fig. S1, F to H; movement offset fig. S3, E and F). We also observed an increase in DRN 5-HT fluorescence on movement onset in escape (failed) trials in the avoidance task (Fig. 2, E and F), during which mice were also in direct contact with the stressor. Finally, we microendoscopically recorded DRN 5-HT activity (20) and observed similar environment-dependent switching of movement dynamics in single DRN 5-HT neurons (fig. S4 and fig. S5). Thus, DRN 5-HT neural activity decreases on movement initiation in low- or moderate-threat environments, but high threat, escape-provoking environments invert this response.

To probe the causal role of DRN 5-HT neurons in regulating movement in different environments, we optogenetically (21) activated 5-HT neurons (Fig. 3A and fig. S6A) during these behaviors. Optical stimulation of DRN 5-HT neurons reduced speed in the OFT (Fig. 3, B and C, ChR2 3.67+/− 0.31 cm/s versus eYFP 5.16 +/− 0.44 cm/s), as expected (10). Speed decreased upon stimulation in both approach and avoidance tasks (Approach: Fig. 3, D and E, and fig. S6, B and C, ChR2 3.0 +/− 0.3 cm/s versus eYFP 7.1 +/− 1.0 cm/s; Avoidance: Fig. 3, G and H, and fig. S6, D and E, ChR2 2.2 +/− 0.4 cm/s versus eYFP 3.8 +/− 0.4 cm/s), and latency to chamber crossing was greater in stimulated animals in both tasks (Fig. 3, F and I). TST stimulation in the same mice produced an increase in movement (Fig.

3, J to L). These data provide causal evidence for a switch in DRN 5-HT neuron function from suppression to facilitation of movement in high-threat escape conditions.

We then investigated the movement-related dynamics of DRN GABA neurons using fiber photometry in Vgat-ires-Cre mice (22) (fig. S7, A and B, and fig. S8). Activity decreased on movement to cross the chamber in the approach task (Fig. 4, A to C; movement offset, fig. S3, G and H) but increased on movement to cross the chamber in the avoidance task (Fig. 4, F to H; movement offset, fig. S3, I and J), switching at a lower threat level than DRN 5-HT neurons. Recordings during avoidance training revealed rapid switching following the first few shocks (fig. S9 and fig. S10).

Approach and avoidance differ in environmental valence, and we found that movement-related dynamics also switched in other valenced environments. Wheel running (Fig. 4K) induced a reduction in DRN GABA activity (Fig. 4, L to N; GFP data, Fig. 4N and fig. S7, C to E), but DRN GABA neural activity increased on movement during the TST (Fig. 4, P to S, GFP data, Fig. 4S and fig. S7, F to H; movement offset fig. S3, K and L) and on movement in escape (failed) trials in the avoidance task (fig. S7, I to L).

Finally, we investigated if DRN GABA neurons have a causal role in movement regulation. Optogenetic stimulation of GABA DRN neurons (fig. S11, A and B) had no impact on either speed (Fig. 4, D and E, and fig. S11, C and D, ChR2 7.3 +/− 0.7 m/s versus eYFP 6.7 +/− 1.0 m/s) or latency to chamber crossing (fig. S11E) in the approach task or on wheel mobility (Fig. 4O), but stimulation in these same mice induced higher speed in the OFT (fig. S12, A to D). Stimulation increased speed (Fig. 4, I and J and fig. S11, F and G, ChR2 7.7 +/− 0.7 m/s versus eYFP 4.0 +/− 0.2 m/s) and reduced latency (fig. S11H) in the avoidance task, and increased movement in the TST (Fig. 4T), revealing a causal role for DRN GABA neurons in promoting movement in environments with negative valence.

These findings demonstrate that changes in environmental threat intensity and valence switch the functional roles of DRN 5-HT and GABA neurons in movement regulation. The notion that movement in states of extreme threat may be differently regulated is not without precedent. Paradoxical kinesia has been observed in akinetic Parkinsonian patients (23), and DA-depleted akinetic rats attempt escape in deep water (24), suggesting alternate motor regulation in fight-or-flight situations. DRN function during stress is regulated by a number of systems that may play a role in environment-dependent functional switching; SSRI-induced TST immobility reduction requires DRN norepinephrine (25); DRN corticotropin-releasing factor inhibits 5-HT release and promotes active coping or the reverse depending on stress history (26, 27); and DRN activation is dampened by prefrontal activity during controllable stress (28).

Here, we have probed the neural dynamics and functional roles of two distinct DRN cell types in movement regulation. Urgent escape conditions switch DRN 5-HT neurons from suppression of movement to facilitation, and DRN GABA neurons selectively facilitate movement in environments with negative valence, consistent with the neural dynamics of both cell types. These results reveal a role for DRN circuits in rapid, environment-specific behavioral regulation.

Supplementary Material

Refer to Web version on PubMed Central for supplementary material.

Acknowledgments

We thank T.J. Davidson and C.B. Schaffer for photometry advice; P. Dayan, I.T. Ellwood, R.M. Harris-Warrick, R.R. Hoy, J.H. Goldberg, J.R. Fetcho, E. Troconis, and D.A. Bulkin for helpful discussions and/or comments on the manuscript; T. Bollu for technical advice; G. Paquelet for microendoscopy advice; U. Lee for contributions to figure design; A.K. Recknagel for expert technical assistance; and the Warden laboratory and Cornell Neurobiology and Behavior for training and support.

Funding: Supported by the Mong Family Foundation (C.S., Y.Y.H., A.G.), the Taiwan Ministry of Education (Y.Y.H), NIH DP2MH109982 (M.R.W), the Alfred P. Sloan Foundation (M.R.W.), the Whitehall Foundation (M.R.W.), and the Brain and Behavior Research Foundation (M.R.W). M.R.W. is a Robertson Neuroscience Investigator–New York Stem Cell Foundation.

References and Notes

1. Fanselow MS, Neural organization of the defensive behavior system responsible for fear. Psychon. Bull. Rev 1, 429–38 (1994). [PubMed: 24203551]
2. De Franceschi G, Vivattanasarn T, Saleem AB, Solomon SG, Vision Guides Selection of Freeze or Flight Defense Strategies in Mice. Curr. Biol 26, 2150–4 (2016). [PubMed: 27498569]
3. Ydenberg RC, Dill LM, The economics of fleeing from predators. Adv. Study Behav 16, 229–249 (1986).
4. Ogawa SK, Cohen JY, Hwang D, Uchida N, Watabe-Uchida M, Organization of monosynaptic inputs to the serotonin and dopamine neuromodulatory systems. Cell Rep. 8, 1105–18 (2014). [PubMed: 25108805]
5. Niv Y, Daw ND, Joel D, Dayan P, Tonic dopamine: opportunity costs and the control of response vigor. Psychopharmacology (Berl). 191, 507–20 (2007). [PubMed: 17031711]
6. Salamone JD et al., Mesolimbic dopamine and the regulation of motivated behavior. Curr. Top. Behav. Neurosci 27, 231–57 (2016). [PubMed: 26323245]
7. Soubrié P, Reconciling the role of central serotonin neurons in human and animal behavior. Behav. Brain Sci 9, 319 (1986).
8. Deakin JFW, Graeff FG, 5-HT and mechanisms of defence. J. Psychopharmacol 5, 305–15 (1991). [PubMed: 22282829]
9. Miyazaki KW et al., Optogenetic activation of dorsal raphe serotonin neurons enhances patience for future rewards. Curr. Biol. 24, 2033–40 (2014). [PubMed: 25155504]
10. Correia PA et al., Transient inhibition and long-term facilitation of locomotion by phasic optogenetic activation of serotonin neurons. Elife. 6, 1–26 (2017).
11. Marcinkiewcz CA et al., Serotonin engages an anxiety and fear-promoting circuit in the extended amygdala. Nature. 537, 97–101 (2016). [PubMed: 27556938]
12. Harrison AA, Everitt BJ, Robbins TW, Central 5-HT depletion enhances impulsive responding without affecting the accuracy of attentional performance: Interactions with dopaminergic mechanisms. Psychopharmacology (Berl). 133, 329–342 (1997). [PubMed: 9372531]
13. Clarke HF, Dalley JW, Crofts HS, Robbins TW, Roberts AC, Cognitive inflexibility after prefrontal serotonin depletion. Science. 304, 878–80 (2004). [PubMed: 15131308]
14. Cryan JF, Markou A, Lucki I, Assessing antidepressant activity in rodents: recent developments and future needs. Trends Pharmacol. Sci 23, 238–245 (2002). [PubMed: 12008002]
15. Warden MR et al., A prefrontal cortex–brainstem neuronal projection that controls response to behavioural challenge. Nature. 492, 428–432 (2012). [PubMed: 23160494]
16. Gunaydin LA et al., Natural neural projection dynamics underlying social behavior. Cell. 157, 1535–51 (2014). [PubMed: 24949967]
17. Chen T-W et al., Ultrasensitive fluorescent proteins for imaging neuronal activity. Nature. 499, 295–300 (2013). [PubMed: 23868258]

18. Zhuang X, Masson J, Gingrich JA, Rayport S, Hen R, Targeted gene expression in dopamine and serotonin neurons of the mouse brain. J. Neurosci 143, 27–32 (2005).
19. Commons KG, Cholanians AB, Babb JA, Ehlinger DG, The rodent forced swim test measures stress-coping strategy, not depression-like behavior. ACS Chem. Neurosci 8, 955–960 (2017). [PubMed: 28287253]
20. Ziv Y et al., Long-term dynamics of CA1 hippocampal place codes. Nat. Neurosci 16, 264–6 (2013). [PubMed: 23396101]
21. Boyden ES, Zhang F, Bamberg E, Nagel G, Deisseroth K, Millisecond-timescale, genetically targeted optical control of neural activity. Nat. Neurosci 8, 1263–8 (2005). [PubMed: 16116447]
22. Vong L et al., Leptin action on GABAergic neurons prevents obesity and reduces inhibitory tone to POMC neurons. Neuron. 71, 142–54 (2011). [PubMed: 21745644]
23. Bonanni L, Thomas A, Onofrj M, Paradoxical kinesia in parkinsonian patients surviving earthquake. Mov. Disord 25, 1302–4 (2010). [PubMed: 20310034]
24. Marshall JF, Levitan D, Stricker EM, Activation-induced restoration of sensorimotor functions in rats with dopamine-depleting brain lesions. J. Comp. Physiol. Psychol 90, 536–46 (1976). [PubMed: 8470]
25. O'Leary OF, Bechtholt AJ, Crowley JJ, Valentino RJ, Lucki I, The role of noradrenergic tone in the dorsal raphe nucleus of the mouse in the acute behavioral effects of antidepressant drugs. Eur. Neuropsychopharmacol 17, 215–26 (2007). [PubMed: 16997535]
26. Waselus M, Nazzaro C, Valentino RJ, Van Bockstaele EJ, Stress-induced redistribution of corticotropin-releasing factor receptor subtypes in the dorsal raphe nucleus. Biol. Psychiatry 66, 76–83 (2009). [PubMed: 19362706]
27. Puglisi-Allegra S, Andolina D, Serotonin and stress coping. Behav. Brain Res 277, 58–67 (2015). [PubMed: 25108244]
28. Amat J et al., Medial prefrontal cortex determines how stressor controllability affects behavior and dorsal raphe nucleus. Nat. Neurosci 8, 365–71 (2005). [PubMed: 15696163]

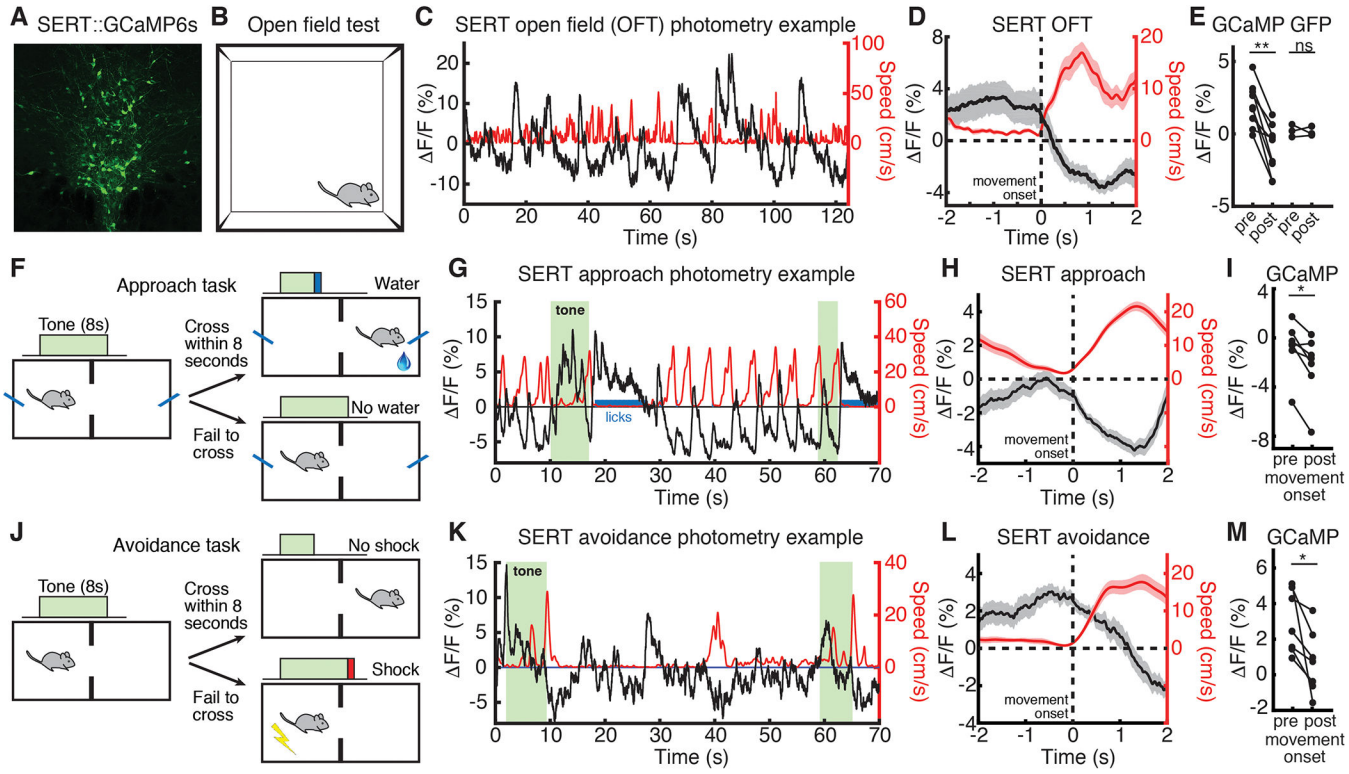

Fig. 1. DRN 5-HT neural activity decreases upon movement in low- or moderate-threat environments.

(**A**) GCaMP6s expression in DRN 5-HT neurons in a SERT-Cre mouse. (**B**) OFT schematic. (**C**) Example OFT photometry from a SERT::GCaMP6s mouse. GCaMP ΔF/F in black, speed in red. (**D**) Mean ΔF/F aligned to OFT movement onset. (**E**) Mean ΔF/F before and after OFT movement onset in GCaMP (n=9) and GFP (n=3) mice. (**F**) Approach task schematic. (**G**) Example approach photometry from the same mouse. (**H**) Mean ΔF/F aligned to approach movement onset. (**I**) Mean ΔF/F before and after approach movement onset in GCaMP (n=7) mice. (**J**) Avoidance task schematic. (**K**) Example avoidance photometry data from the same mouse. (**L**) Mean ΔF/F aligned to avoidance movement onset. (**M**) Mean ΔF/F before and after avoidance movement onset in GCaMP (n=7) mice. $*P < 0.05$, $**P < 0.01$, Wilcoxon signed-rank test. Error bars indicate s.e.m.

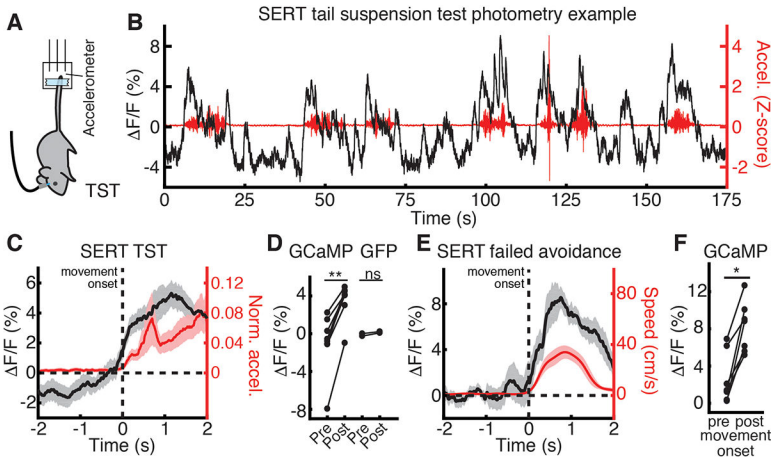

Fig. 2. DRN 5-HT neural activity increases upon movement in high-threat environments.

(**A**) TST schematic. (**B**) Example TST photometry from the Fig. 1 mouse. GCaMP ΔF/F in black, movement in red. (**C**) Mean ΔF/F aligned to TST movement onset. (**D**) Mean ΔF/F before and after TST movement onset in GCaMP (n=8) and GFP (n=2) mice. (**E**) Mean ΔF/F aligned to escape movement onset during failed avoidance trials. (**F**) Mean ΔF/F before and after escape movement onset in GCaMP (n=7) mice. *$P < 0.05$, **$P < 0.01$, Wilcoxon signed-rank test. Error bars indicate s.e.m.

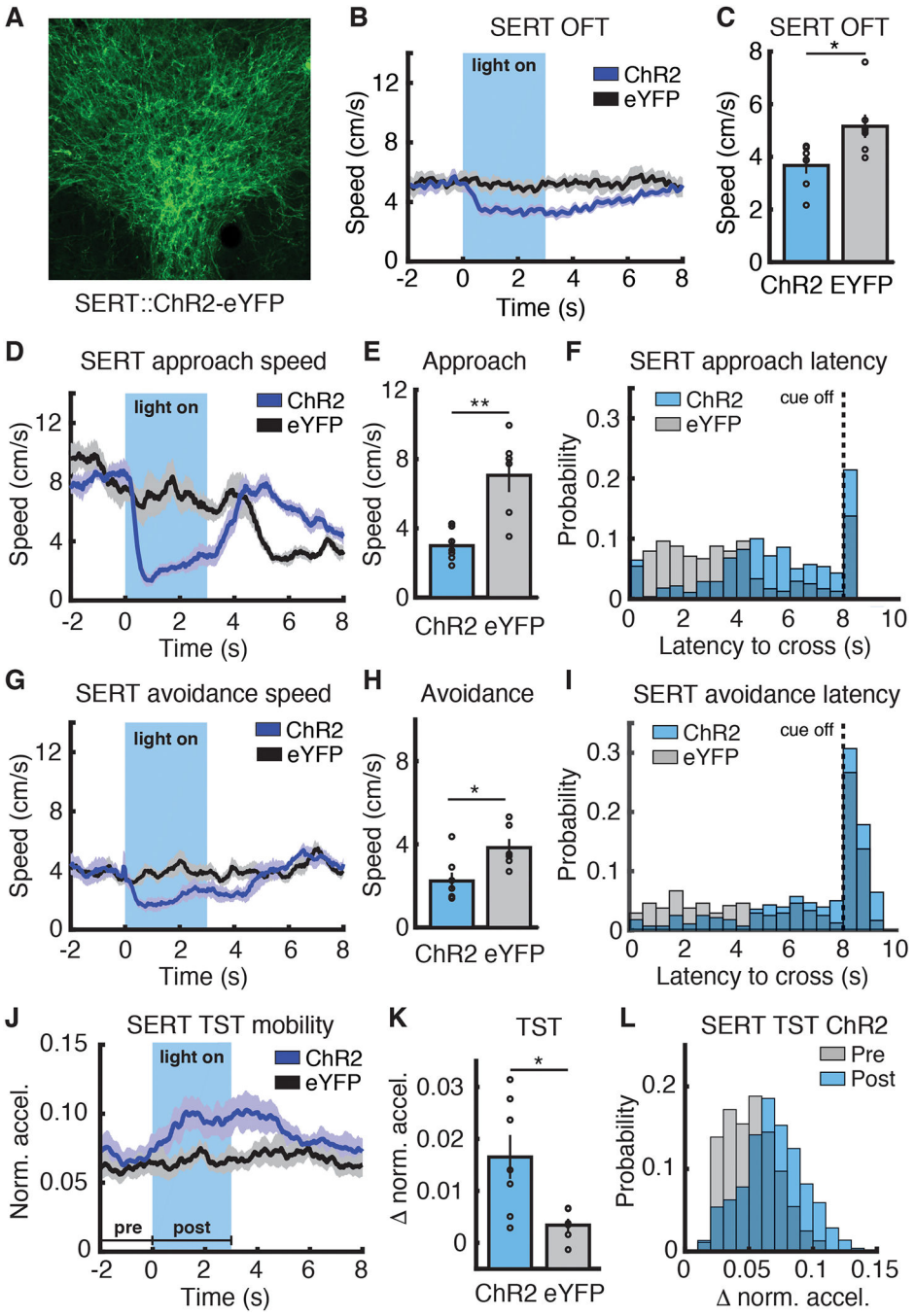

Fig. 3. DRN 5-HT stimulation suppresses or promotes movement at different threat levels.

(**A**) ChR2-eYFP expression in DRN 5-HT neurons in a SERT-Cre mouse. (**B**) Speed aligned to light onset, OFT (SERT::ChR2-eYFP, n=7; SERT::eYFP, n=7). (**C**) Mean speed during stimulation, OFT. (**D**) Speed aligned to light/cue onset, approach task (SERT::ChR2-eYFP, n=7; SERT::eYFP, n=6). (**E**) Mean speed during stimulation, approach task. (**F**) Latency to cross, approach task. $P < 0.0001$, log-rank test. (**G**) Speed aligned to light/cue onset, avoidance task (SERT::ChR2-eYFP, n=7; SERT::eYFP, n=6). (**H**) Mean speed during stimulation, avoidance task. (**I**) Latency to cross distribution, avoidance task. $P < 0.0001$,

log-rank test. (**J**) Movement aligned to light onset, TST (SERT::ChR2-eYFP, n=7; SERT::eYFP, n=6). (**K**) Mean difference between pre- and post-light onset movement, TST. (**L**) SERT::ChR2-eYFP movement before and after light onset, TST. *$P < 0.05$, **$P < 0.01$, Wilcoxon rank-sum test. Error bars indicate s.e.m.

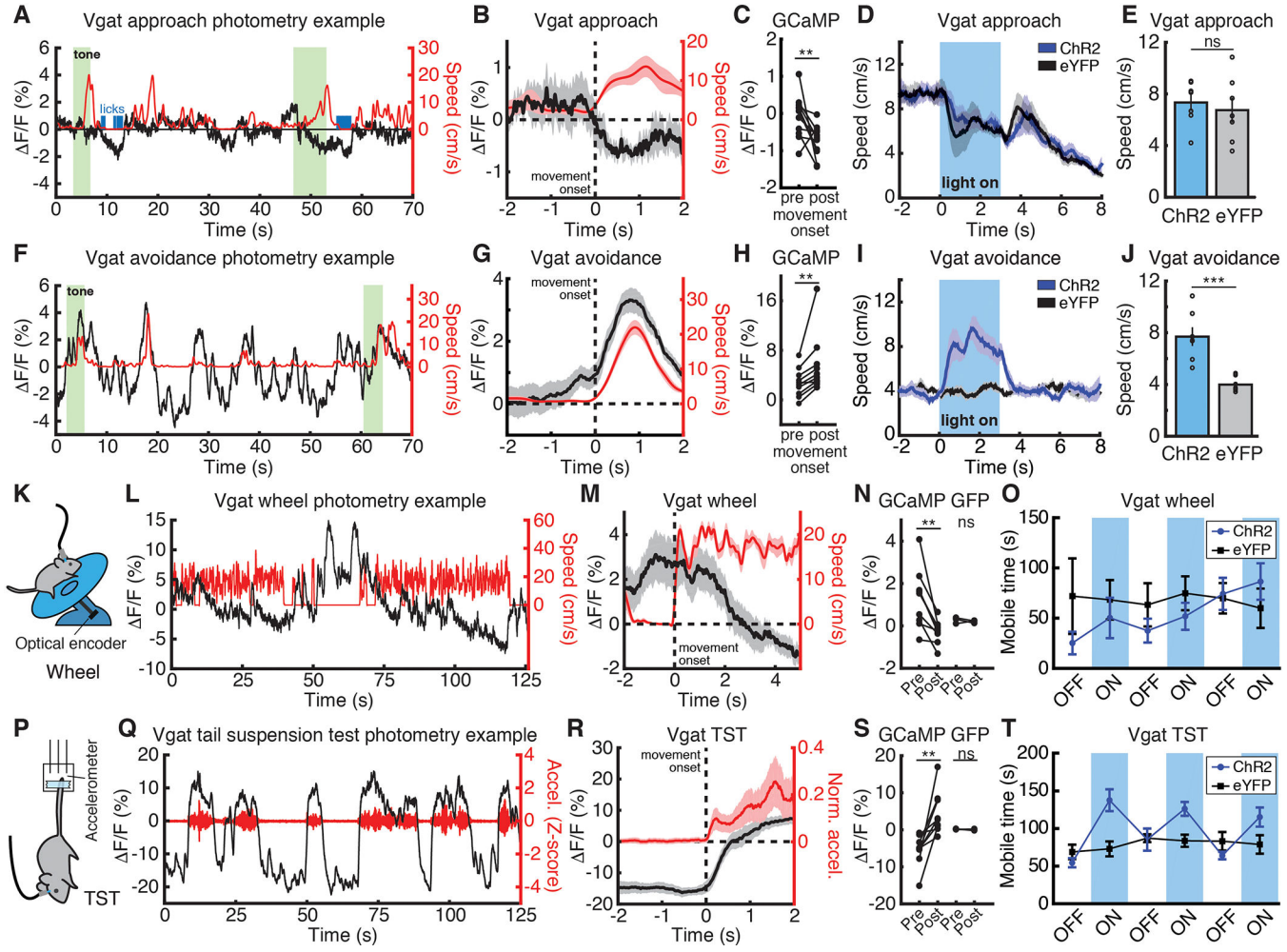

Fig. 4. DRN GABA stimulation promotes movement in environments with negative valence.

(**A**) Approach photometry example from a Vgat::GCaMP6s mouse. GCaMP ΔF/F in black, speed in red. (**B**) Mean ΔF/F aligned to approach movement onset. (**C**) Mean ΔF/F before and after approach movement onset (n=11). (**D**) Speed aligned to stimulation/cue onset, approach (Vgat::ChR2-eYFP, n=8; Vgat::eYFP, n=7). (**E**) Mean speed during stimulation, approach. (**F**) Example avoidance photometry. (**G**) Mean ΔF/F aligned to avoidance movement onset. (**H**) Mean ΔF/F before and after avoidance movement onset (n=10). (**I**) Speed aligned to stimulation/cue onset, avoidance (Vgat::ChR2-eYFP, n=8; Vgat::eYFP, n=7). (**J**) Mean speed during stimulation, avoidance. (**K**) Wheel schematic. (**L**) Example wheel photometry. (**M**) Mean ΔF/F aligned to wheel movement onset. (**N**) Mean ΔF/F before and after wheel movement onset in GCaMP (n=9) and GFP (n=3) mice. (**O**) Mean mobile time in 3-minute stimulation or non-stimulation blocks, wheel (Vgat::ChR2-eYFP, n=7; Vgat::eYFP, n=7; $P = 0.9015$, Wilcoxon rank-sum test). (**P**) TST schematic. (**Q**) TST photometry example. (**R**) Mean ΔF/F aligned to TST movement onset. (**S**) Mean ΔF/F before and after TST movement onset in GCaMP (n=9) and GFP (n=3) mice. (**T**) Mean mobile time in 3-minute stimulation or non-stimulation blocks, TST (Vgat::ChR2-eYFP, n=7; Vgat::eYFP, n=7; $P = 0.007$, Wilcoxon rank-sum test). $^{**}P < 0.01$, $^{***}P < 0.001$

Wilcoxon signed-rank test (photometry) or Wilcoxon rank-sum test (optogenetics). Error bars indicate s.e.m.